Time gating of heralded single photons for atomic memories

B. Melholt Nielsen, J. S. Neergaard-Nielsen, and E. S. Polzik*

Niels Bohr Institute, Danish National Research Foundation Center for Quantum Optics (QUANTOP), Blegdamsvej 17, DK-2100 Copenhagen, Denmark

**Corresponding author: polzik@nbi.dk*

Received September 2, 2009; revised November 16, 2009; accepted November 16, 2009; posted November 24, 2009 (Doc. ID 116279); published December 10, 2009

We demonstrate a method for time gating the standard heralded cw spontaneous parametric downconverted single-photon source by using pulsed pumping of an optical parametric oscillator below threshold. The narrow bandwidth, high purity, high spectral brightness, and pseudodeterministic character make the source highly suitable for light-atom interfaces with atomic memories. © 2009 Optical Society of America

OCIS codes: 270.0270, 270.5290, 270.5530, 270.6570, 030.5260, 190.4970.

In quantum communication and quantum information processing, light is the natural agent for carrying information, whereas atomic systems are highly suitable for storing and processing information. An efficient exchange of quantum information between photonic carriers and atomic nodes becomes important, since it would allow for the implementation of quantum information networks.

In a number of approaches to quantum memory [1], such as electromagnetically induced transparency [2,3], Faraday interaction with feedback [4], and teleportation [5], the temporal mode of the quantum field of interest has to be matched well with that of a strong driving field to achieve a successful storage. An attractive light source for such atomic memories would be the one that generates pure nonclassical quantum states in a deterministic manner.

Single-photon sources based on single emitters in free space usually suffer from poor collection efficiency. This deficiency can be remedied by placing them inside optical cavities [6–8]. Atomic ensembles can serve as sources of single photons [2,3,9]; however, the efficiency to date is not very high. The highest-purity single-photon sources to date are based on heralded spontaneous parametric downconversion (SPDC), where one of the two downconverted photons is counted and heralds the presence of the other photon. The SPDC sources come in a pulsed free-space version [10–13] and in a cavity-enhanced cw setting based on an optical parametric oscillator (OPO) [14]. The narrow bandwidth, perfect spatial mode, and high spectral brightness of the cavity-enhanced setting makes it well suited for application with atomic memories. One major disadvantage of the cw OPO setting is the random character of the state generation.

In this Letter we demonstrate how to generate high-purity time-gated single photons using a pulsed OPO pump in the cw SPDC setup, thus combining the superior spectral and spatial properties of the OPO output with the enhanced regularity of the pulsed-pump approach. The OPO pump pulses impose a gating condition on the single-photon production, whereby the creation of photons inside the OPO cavity is possible only within the time window of the pump pulses. The particular time gates in which the SPDC photon actually appears are heralded by the idler photon. One can thus synchronize the source with the driving field of an atomic memory protocol and then only keep the result in the memory if the heralding photon has been counted. In our experiment we perform a tomographic reconstruction of the single photon using a pulsed temporal mode function, a cw local oscillator (LO), and a homodyne detector (HD).

A master beam is derived from a cw Ti:sapphire laser running at the cesium D2 line ω, as shown in Fig. 1. This beam is split to pump the second-harmonic generator (SHG) and to serve for the production of a blueshifted beam at ω_+ and a redshifted beam at ω_-. Both are shifted by one OPO free spectral range ω_{FSR} to match the first nondegenerate components of the OPO output at $\omega_\pm = \omega \pm \omega_{\mathrm{FSR}}$. The redshifted beam is used as a locking beam for the OPO, the split-off cavity (SC), and the linear filter cavities (FCs), while the blueshifted beam is used as an LO for the homodyne detector. The OPO pump is pulsed using a pulse shaper (PLS), and the generated photon pairs are split on the SC. The photon created at ω_- is transmitted and spectrally filtered using the FC before impinging on the avalanche photodiode (APD), whereby heralding the presence of its twin photon created at ω_+. The twin photon is reflected off the SC and sent onto the HD for tomography. More details can be found in [14].

The PLS is a Pockels cell driver (BME Bergmann) with a KD*P Pockels cell and a polarizing beam split-

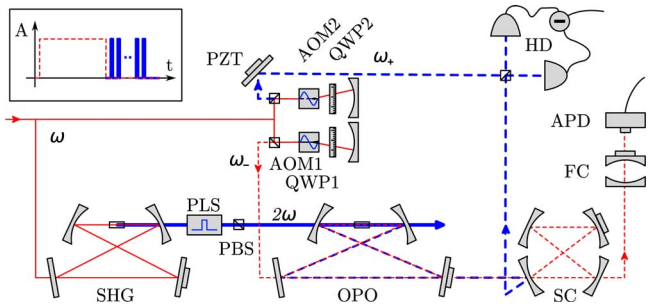

Fig. 1. (Color online) Experimental setup. Inset, experimental cycle of locking and pulsing.

ter (PBS). The maximum repetition rate is 200 kHz, and the optical rise time is 5 ns. The pulse extinction ratio is 1.5×10^{-2}, which is mainly due to the poor quality of the PBS. The pulse length is controlled by electronically delaying the signal that turns the pulse off.

Within one experimental cycle we first dither the length of the OPO, the SC, and the FC around their resonances using the redshifted beam as a locking beam and monitoring the APD signal to tune all cavities to resonance. When the cavities are on resonance we turn off the redshifted beam with the acousto-optical modulator (AOM1) and let them stand passively while pulsing the OPO pump with a 50 kHz repetition rate during the measurement (see inset in Fig. 1). We measure for 200 ms and lock for 800 ms. The OPO, the SC, and the FC are able to passively stay near resonance for up to 10 s.

We first measure the photon-counting distribution of the field arriving at the APD. This is done using a digital oscilloscope (Lecroy Wavepro 7100) to record the time delay of the APD counts occurring within 500 ns of the front of the electronic pulse driving the PLS. Histograms of measured APD click delay times for three different optical pulse lengths are shown in the inset of Fig. 2. The raw count rates are 4.4 s^{-1}, 5.7 s^{-1}, and 27 s^{-1} for pulses of length 7 ns, 20 ns, and 49 ns. Without pulsing the corresponding rate is 275 s^{-1}. The background count rate is 3.8 s^{-1} and is mainly due to the poor extinction ratio of the PLS, since the APD dark count is 0.4 s^{-1}. It should be possible to improve the count rate by increasing the repetition rate and measurement time window.

To model the photon-counting distribution we consider propagation of the optical pulse through the OPO, the SC, and the FC. The pulse was a square with the rise time of 5 ns, and the field transmission through a cavity corresponds to applying a Lorentzian frequency filter,

$$F(\omega) \propto \frac{\kappa}{\kappa^2 + \omega^2}, \tag{1}$$

where κ is half the cavity bandwidth. The output field is found by convolution,

$$z(t) \propto \int_{-\infty}^{t} z_p(\tau) F(t-\tau)\mathrm{d}\tau, \tag{2}$$

where $z_p(t)$ is the temporal profile of the pulse and $F(t)$ is the time-domain response of the product of the frequency filters of the OPO, $\gamma/2\pi=4.4$ MHz, and the most narrow filter cavity, $\kappa/2\pi=12$ MHz. This rough model is compared with the APD count data in Fig. 2. The data have been scaled vertically by the same factor to fit the model, and the background level has been removed.

The homodyne measurement is done using the oscilloscope to record homodyne data conditioned on an APD click occurring within a 40-ns-long acceptance window, as shown in Fig. 3. The acceptance window is centered on the time of the peak of the photon-count distribution. On every click we sample a 500-ns-long window from the front edge of the electronic pulse. The sample rate is 10^9 s^{-1}, and we collect data from a few 10^4 clicks.

We estimate the temporal mode function for postprocessing the homodyne data by looking at the variance of the individual points between successive time windows—see Fig. 4 for the case of a 49-ns-long pulse. The noise variance has been normalized to the vacuum level and filtered using a 25 MHz low-pass filter to remove some high-frequency electronic noise due to the experimental hardware. The ripples after the peak in Fig. 4 are electronic noise from the APD, and the additional time delay compared with that of Fig. 2 is due to the difference in the optical and electronic paths.

In [15] the task of finding the optimal mode function for the pulsed pump setting is addressed. There it is shown that, in the limit where the acceptance window is much longer than the round-trip time of the OPO, a good approximation for the optimal mode function is the temporal profile of the pulse convoluted by the OPO filter. Since our round-trip time is 2.7 ns we are roughly in that limit with a 40-ns-long acceptance window. A comparison of this optimal mode function with the experimental noise variance is given in Fig. 4.

The postprocessing is done by multiplying the data from each time window by the mode function and in-

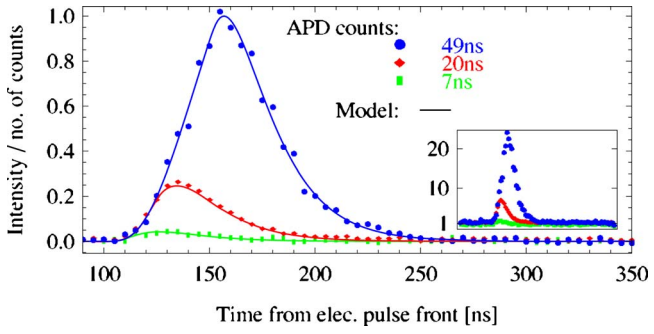

Fig. 2. (Color online) Photon-counting distribution, comparing model, and data. The solid curves are model output through the OPO, the SC, and the FC. Points, rescaled APD count data. Inset, the 500-ns-long raw distribution normalized to the background level.

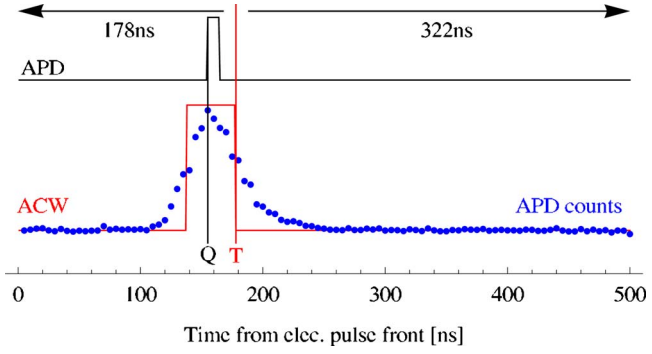

Fig. 3. (Color online) Homodyne data acquisition. The APD click serves as a qualifier (Q). The trailing edge of the acceptance window (ACW) serves as a trigger (T) if and only if it occurs within 40 ns after the qualifier. An APD count distribution is shown for comparison.

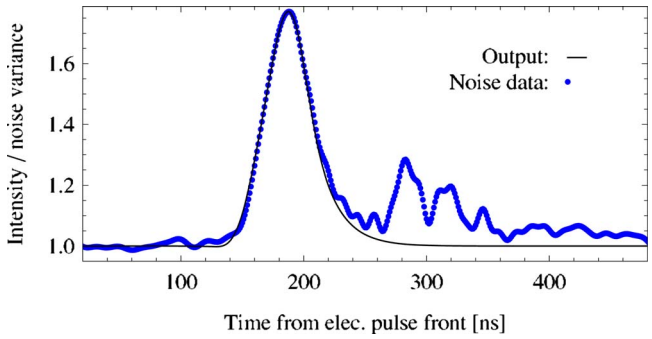

Fig. 4. (Color online) Noise variance of 13,000 time windows for a 49-ns-long pulse. The solid curve is a model pulse filtered by the OPO and low-pass filtered for comparison.

tegrating to obtain one quadrature point. These quadrature points are then normalized to a vacuum level. Assuming the generated state to be phase invariant we use all the quadrature points to obtain the phase-averaged marginal distribution shown in Fig. 5.

We take the generated state to be a sum of Fock states $n=0,1,\ldots,6$ and fit this model to the marginal distribution. The best fit is shown in Fig. 5. The first three diagonal elements of the density matrix are $\rho_{00}=0.392$, $\rho_{11}=0.595$, and $\rho_{22}=0.010$, while the rest are of order 10^{-3} or less. The center value of the Wigner function is $W(0,0)=(\rho_{00}-\rho_{11}+\rho_{22}-\cdots)/\pi$, and using the above diagonal elements it evaluates to $W(0,0)=-0.061$. It should be noted that these numbers have not been corrected for any experimental inefficiencies.

A similar homodyne measurement using a 20-ns-long pump pulse resulted in a somewhat worse generated single-photon state, although it should have been better because of a better-defined temporal mode according to [15]. The first two diagonal elements of the phase-averaged density matrix of 4200 quadrature points are $\rho_{00}=0.542$ and $\rho_{11}=0.458$, while the rest are vanishingly small. The center value of the Wigner function for these diagonal elements is $W(0,0)=0.027$. We believe the reason for this is the background level visible in the inset of Fig. 2. The "signal-to-noise" ratio is worse for the 20 ns pump than for the 49 ns pump, and this implies that we sample more vacuum and less single photons.

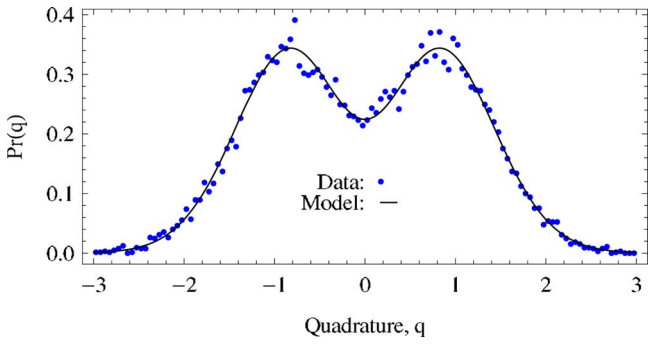

Fig. 5. (Color online) Marginal distribution of 13,000 quadrature points. The points are the phase-averaged marginal distribution, and the solid curve is the model fit.

The source presented here is of high purity comparable to the two SPDC-based sources with the highest purity reported to date in [12] (pulsed, purity 80%, rate 1,000 s^{-1}, bandwidth 5 THz) and in our earlier work [14] (cw, purity 70%, rate 13,000 s^{-1}, bandwidth 8 MHz). Its spectral brightness is 10^4 times higher than that of the free-space source [12]. The spectral brightness reported here is 500 times lower than that of the heralded cw source [14], which is the price we pay for the gated character of the present source.

In summary, we have demonstrated the improved regularity of the heralded cw SPDC single-photon source by time gating the photon-pair production using the pulsed pumping of the OPO. The time gating makes it possible to synchronize the single photon with atomic memory protocols by choosing the driving field pulse for the memory interaction according to the suitable temporal mode function. The generated single photons have a bandwidth of a few megahertz suitable for atomic memories, a well-defined spatial mode, high purity, and high spectral brightness.

This research was funded by European grants Qubit Applications Project (QAP), Computing with Mesoscopic Photonic and Atomic States (COMPAS), and Engineering, Manipulation and Characterization of Quantum States of Matter and Light (EMALI).

References

1. K. Hammerer, A. S. Sørensen, and E. S. Polzik, arXiv:org quant-ph/0807.3358 (2008).
2. M. Eisaman, A. Andre, F. Massou, M. Fleischhauer, A. Zibrov, and M. Lukin, Nature **438**, 837 (2005).
3. T. Chaneliere, D. N. Matsukevich, S. Jenkins, S. Y. Lan, T. A. B. Kennedy, and A. Kuzmich, Nature **438**, 833 (2005).
4. B. Julsgaard, J. Sherson, J. I. Cirac, J. Fiurášek, and E. S. Polzik, Nature **432**, 482 (2004).
5. J. Sherson, H. Krauter, R. K. Olsson, B. Julsgaard, K. Hammerer, I. Cirac, and E. S. Polzik, Nature **443**, 557 (2006).
6. J. McKeever, A. Boca, A. D. Boozer, R. Miller, J. R. Buck, A. Kuzmich, and H. J. Kimble, Science **303**, 1992 (2004).
7. M. Pelton, C. Santori, J. Vukovic, B. Zhang, G. S. Solomon, J. Plant, and Y. Yamamoto, Phys. Rev. Lett. **89**, 233602 (2002).
8. T. Legero, T. Wilk, M. Hennrich, G. Rempe, and A. Kuhn, Phys. Rev. Lett. **93**, 070503 (2004).
9. C. Chou, S. Polyakov, A. Kuzmich, and H. J. Kimble, Phys. Rev. Lett. **92**, 213601 (2004).
10. A. I. Lvovsky, H. Hansen, T. Aichele, O. Benson, J. Mlynek, and S. Schiller, Phys. Rev. Lett. **87**, 050402 (2001).
11. A. Zavatta, S. Viciani, and M. Bellini, Phys. Rev. A **70**, 053821 (2004).
12. T. B. Pittman, B. C. Jacobs, and J. D. Franson, Opt. Commun. **246**, 545 (2006).
13. A. Ourjoumtsev, R. Tualle-Brouri, J. Laurat, and P. Grangier, Phys. Rev. Lett. **96**, 213601 (2006).
14. J. S. Neergaard-Nielsen, B. M. Nielsen, H. Takahashi, A. I. Vistnes, and E. S. Polzik, Opt. Express **15**, 7940 (2007).
15. A. E. B. Nielsen and K. Mølmer, Phys. Rev. A **76**, 033832 (2007).